

23 **Abstract**

24 *Salmonella spp.* is one of the top foodborne pathogens associated with low-moisture foods and
25 they exhibit significant resistance to conventional thermal treatments. UV light pulses emitted
26 from light emitting diode (LED) has shown antimicrobial potential in high-moisture foods and
27 water. However, limited information is available about the antimicrobial potential of UV light with
28 different wavelengths, including 395 nm in low-moisture foods. The objectives of this study were
29 to investigate the antimicrobial potential of 395 nm pulsed LED light in wheat flour and the
30 resulting quality changes. This study demonstrated a maximum 2.91 log reduction of *Salmonella*
31 cocktail in wheat flour treated with 395 nm pulsed LED for 60 min in a semi-closed system.
32 Oxidation occurred in wheat flour after 30 and 60 min exposure to the 395 nm LED, which
33 subsequently led to bleaching, and polymerization of gluten components through disulphide
34 linkage. The water holding capacity of gluten was reduced by oxidation, and the contents of
35 secondary structures were altered significantly after pulsed LED treatment, but the rheological
36 properties were not deteriorated. The disulfide bond formation naturally happens during dough
37 formation and the oxidation triggered by pulsed LED treatment may play a role on accelerating
38 this process. The 395 nm pulsed LED treatment could be a promising decontamination technology
39 for wheat flour with an additional benefit of bleaching of the flour without chemicals.

40

41 **Industrial relevance**

42 A number of foodborne outbreaks and recalls have been related to low-moisture foods in these
43 decades and recently several outbreaks were reported due to the occurrence of *Salmonella* in wheat
44 flour. However, it is difficult to solve this problem through conventional thermal approaches
45 because of the increased thermal resistance of *Salmonella* at low water activity environment. The
46 emerging LED light source can produce light with monochromatic wavelengths without the use of
47 mercury vapor lamps. It also has high durability, low heat generation, and is relatively easy to be
48 adapted in an existing production line. Therefore, there is a great potential of using certain UV
49 wavelengths emitted from LED to disinfect the low-moisture foods in food industries. To the best
50 of our knowledge, no research was conducted on decontamination of wheat flour by using LEDs
51 and only limited studies are available on the influence of pulsed LED treatment on food quality.
52 The aim of this study was to explore the possibility of using 395 nm pulsed LED treatment as a
53 novel tool for decontamination of *Salmonella* in a low-moisture food product (wheat flour) with
54 industrial feasibility, and investigate the influence of the pulsed LED treatment on quality changes
55 in the product.

56

57 **Highlights**

- 58 • The 395 nm pulsed LED resulted 2.9 log reduction of *Salmonella spp.* in wheat flour
- 59 • Bleaching and oxidation occurred in wheat flour with 395 nm LED treatment
- 60 • LED treatment induced polymerization of gluten proteins through disulphide linkage
- 61 • The elastic property of gluten was enhanced by LED
- 62 • Contents of intermolecular β -sheet and β -turn structures were increased

63 **Keywords**

64 Low-moisture foods, wheat flour, *Salmonella*, light emitting diode (LED), UV-A, oxidation

65 **1. Introduction**

66 According to the Government of Canada (2016), about 4 million Canadians are affected by
67 foodborne illnesses every year, and 5% of the cases are attributable to *Salmonella enterica*. In the
68 annual report of CDC (2015), 7719 *Salmonella* infections were confirmed in US and among which
69 535 infections were outbreak-associated. Compared with 2015–2017, the incidence of infection
70 significantly raised 9% for *Salmonella* in 2018 (Tack et al., 2019). Recalls and foodborne illnesses
71 have been increasingly linked to low-moisture foods with water activity (a_w), with $a_w < 0.85$, such
72 as wheat flour, milk powder, dry nuts, spices, and pet foods (Beuchat et al., 2013; CDC 2015;
73 Syamaladevi et al., 2016a; Syamaladevi et al., 2016b). Low-moisture foods are often considered
74 as long shelf-life products with negligible risk to deteriorate, for example, wheat flour usually have
75 a shelf-life from 3 months to 12 months. Contamination of *Salmonella spp.* is one of the top
76 hazards in low-moisture foods, because they can survive for a period of time under low-moisture
77 conditions. In addition, the thermal resistance of *Salmonella* is greatly increased at lower a_w
78 (Archer, Jarvis, Bird and Gaze, 1998; Bari et al., 2009), therefore, *Salmonella* in low-moisture
79 foods is difficult to control by conventional thermal treatments.

80 Light emitting diodes (LED) are semiconductors that emit light in response to electric
81 current (Schubert, 2003). LEDs emitting UV light pulses inactivate microorganisms; in
82 comparison to mercury vapor lamps, LEDs generate less heat, and the light intensity remains
83 constant over the lifetime of the lamp (Shin et al., 2016). UV-C light with wavelength between
84 200-280 nm has been generally used for disinfection purpose. It exhibits high antimicrobial
85 potential and mainly targets on the DNA/RNA damage of bacteria (Beck et al., 2015; Dai et al.,
86 2012). UV-A (315-400 nm) also has photo-bactericidal activity, but acts by different mechanisms
87 because it is not directly absorbed by native DNA (Rastogi, et al., 2010). Notably, the exposure to

88 the UV-B (280-315 nm) and UV-C light can induce sunburn and skin cell damage, while the UV-
89 A is much less hazardous to human eyes and skin (Shirai, Watanabe and Matsuki, 2016).

90 Microbial inactivation by UV-A light is mainly attributed to oxidation of unsaturated
91 membrane fatty acids and the interactions between the UV photons and endogenous
92 photosensitizers of bacteria (Bintsis, Tzanetaki and Robinson, 2000). The photosensitizer in
93 excited state transfers energy to generate reactive oxygen species (ROS) such as peroxides,
94 superoxide, hydroxyl radical and singlet oxygen, and induce oxidative stress, which further results
95 in DNA damage and cell death of microorganisms (Karran and Brem, 2016). The ROS released
96 during this process, however, may also interact with biomolecules in the treated food matrix.
97 Oxidation of the food matrix may affect the functional properties, nutritional and sensory attributes
98 of food products. Therefore, it is necessary to determine whether decontamination treatment with
99 UV-A also changes the quality of the food. Only few studies employed LED sourced UV-A light
100 for inactivation of foodborne pathogens (Shirai, Watanabe and Matsuki, 2016; Haughton et al.,
101 2012). No previous study reported the use of UV-A LED for *Salmonella* inactivation in low-
102 moisture foods or oxidation of the food products after UV-A LED treatments.

103 In recent years, there were several *Salmonella* outbreaks associated with wheat flour and
104 its related products around the world (CDC, 1998; McCallum et al., 2013; Forghani et al., 2019;
105 FDA, 2019). A current study pointed the prevalence of *Salmonella* in wheat flour as well (Myoda
106 et al., 2019). The FDA alerted the public that consuming raw flour and its derivatives showed
107 health risks due to the possibility of *Salmonella* contamination (FDA, 2017). Therefore, it is
108 worthy to investigate the effect of UV-A LED on *Salmonella* contaminated wheat flour. ROS
109 released in the food matrix during the UV-A treatment may oxidize flour components including
110 gluten (consists of gliadin and glutenin proteins), which is the most important functional protein

111 component in wheat flour. The polymerization of glutenin by intermolecular disulfide bonds forms
112 the glutenin macropolymer, a three-dimensional protein network that is the major determinant of
113 the baking quality of wheat (Wieser, 2007). Oxidation of gluten proteins increases the number of
114 inter-molecular disulfide bonds and improve gluten functionality in baking applications (Wieser,
115 2007).

116 The aim of this study was to explore the possibility of using 395 nm pulsed LED treatment
117 as a novel tool for decontamination of the *Salmonella* in wheat flour with industrial feasibility.
118 The functional and structural changes of the gluten proteins in the wheat flour following the 395
119 nm pulsed LED treatment due to possible oxidation were also investigated in this study.

120

121 **2. Materials and Methods**

122 2.1 Materials

123 Unbleached enriched wheat flour (moisture 10.4%, ash 0.62%, protein 10.82%, carbohydrates
124 78.16%) was obtained from P&H Milling Group (Lethbridge, AB, Canada). The initial a_w of the
125 wheat flour was 0.20, measured at 25 °C using a water activity meter (Meter group, Pullman, WA).
126 Five strains of *Salmonella spp.* (ATCC 13311, ATCC 43845 from American Type Culture
127 Collection , FUA 1934, FUA 1946 and FUA 1955) were stored in tryptic soy broth (TSB) and 70%
128 (v/v) glycerol at -80 °C. The *Salmonella enterica* ATCC 13311 and ATCC 43845 were selected
129 to include strains with average and exceptionally high resistance to wet heat (Ng et al., 1969;
130 Mercer et al., 2017). The *Salmonella* FUA 1934, FUA 1946 and FUA 1955 are waste water
131 isolates showing resistance to drying and to dry heat but not to wet heat (cite Bina's thesis). The
132 tryptic soy agar (TSA), TSB, yeast extract and peptone were purchased from Fisher Scientific
133 (Hampton, U.S.). All solvents used in liquid chromatography were high performance liquid

134 chromatography (HPLC) grade, and all other chemicals were of analytical grade. All buffers were
135 prepared with Milli-Q purified water (Millipore, Bedford, MA).

136 2.2 Bacterial culture conditions and cocktail

137 Each frozen *Salmonella* stock culture was streaked on a TSA plate supplemented with 0.6 % (w/v)
138 yeast extract (TSAYE) and incubated for 24 h at 37 °C. A single colony from each plate was picked
139 and cultured in 5 mL of TSB for 24 h at 37 °C, followed by transferring 100 µL into 5 mL TSB
140 (20 h at 37 °C). Then 100 µL of the culture was evenly spread onto a TSAYE plate and the bacterial
141 lawn was harvested with 1.5 mL 0.1% (w/v) peptone water after 24 h incubation at 37 °C (Danyluk,
142 Uesugi and Harris, 2005). Bacterial cells were harvested by centrifugation ($9,632 \times g$, 5 min) and
143 resuspended with 1 mL of peptone water and subjected to another centrifugation. After removing
144 the supernatant, the pellet was suspended again with peptone water to make up to 1 mL total
145 volume. *Salmonella* cocktail (10^{10} CFU/mL) was obtained by mixing all the five 1 ml suspensions
146 and used immediately to inoculate the wheat flour sample.

147 2.3 Inoculation and equilibration of wheat flour

148 The inoculation and equilibration procedures were followed according to Liu et al. (2018) with
149 some modifications. The *Salmonella* cocktail (1.25 mL) was added into 10 g of wheat flour in a
150 sterile polyethylene sampling bag, and then the wheat flour was hand massaged for 3 minutes. The
151 inoculated wheat flour was air-dried for 2 h and then mixed well. Six 0.3 g samples were randomly
152 selected, plated and enumerated on TSAYE plates to confirm the uniformity of inoculum
153 distribution that reached to a final concentration of 10^8 CFU/g. For enumeration, 0.3 g of the
154 sample were mixed with 100 mL of 0.1% (w/v) peptone water and homogenized at 230 rpm for 5
155 min in a Seward Stomacher (Seward, London, UK). Ten milliliters of the suspension were
156 collected, serial diluted, and plated on TSAYE plates in triplicate. The plates were incubated

157 aerobically at 37 °C for 24 h and the number of colonies was counted. Enumeration of background
158 microflora in non-inoculated wheat flour from three random 0.3 g samples was also performed.
159 Before treatment, the a_w of the inoculated wheat flour was equilibrated to 0.75 ± 0.02 in a humidity
160 box filled with saturated sodium chloride solution ($a_w, 25\text{ °C} = 0.75$) for 3 days.

161 2.4 LED systems and inactivation

162 An LED head (111x70x128 mm, JL-3 series, Clearstone, Minnesota, U.S.) consisting of 6 high
163 intensity pulsed LEDs emitting 395 nm light with a built-in cooling fan was connected to a high
164 power pulsed UV LED system (CF3000, Clearstone, Minnesota, U.S.) (Fig. 1A). 0.3 gram of
165 inoculated and equilibrated wheat flour sample was evenly spread over the bottom of the sample
166 cup with a diameter of 3.7 cm and 0.45 mm depth. The sample cup (AquaLab, Pullman, WA, U.S.)
167 was placed under the center of the LED head with a gap of 2 cm. The pulse frequency was 100 Hz,
168 which is the number of pulse periods per unit of time. For inactivation, the power level was selected
169 to 60% with the LED irradiance of 0.45 W/cm^2 , where the ON (t_{ON}) and OFF (t_{OFF}) times of LEDs
170 during pulse period were 6 and 4 milliseconds respectively (Fig. 1B). The emission spectra from
171 the LEDs were determined by StellarNet Inc. spectrometer (Black Comet C-25) (Fig. 1C). The
172 pulsed LED treatments of wheat flour were performed for 0 min, 10 min, 30 min and 60 min. An
173 external fan was used to reduce any temperature increase in the sample during the treatments. The
174 UV dosage values corresponding to the treatment times were determined using a laser energy meter
175 (7Z01580, Starbright, Ophir Photonics, USA). The sample temperature was monitored by
176 attaching a thermocouple in contact with the sample (under LED light) and read at 10 min, 30 min
177 and 60 min. The weight loss was also calculated after treatments.

178 To explore the industrial feasibility of the LED set-up, two conditions were used to perform the
179 LED inactivation. In an open system, the LED set-up was placed in a plastic box that was placed

180 in a biosafety cabinet at ambient temperature and relative humidity. In a semi-closed LED system,
181 the LED set-up was positioned in a controlled humidity chamber with 75% relative humidity and
182 25 °C. The surviving bacterial cells after different LED treatment times were enumerated and
183 compared between both the systems.

184 2.5 Color changes of wheat flour after pulsed LED treatment

185 Color was measured in the wheat flour samples after 0 min, 30 min and 60 min pulsed LED
186 treatments in the semi-closed LED system. The lightness (L^*), redness or greenness (a^*), and
187 yellowness or blueness (b^*) values were obtained using a Minolta CR-400 colorimeter (Konica
188 Minolta Sensing Americas Inc., Ramsey, NJ).

189 2.6 Gluten extraction

190 Wet gluten was extracted from the wheat flour samples based on the method of Kieffer et al. (2007).
191 Two grams of untreated or treated wheat flour sample was mixed with 1 mL of 0.4 M NaCl solution.
192 After resting for 5 min, the dough was washed manually with 20 mL 0.4 M NaCl solution and this
193 step was repeated 5 times until a cohesive matrix was obtained. The gluten was then washed with
194 distilled water to remove the salt, followed by centrifugation at $5,320 \times g$ for 10 min. Dry gluten
195 powder was obtained after lyophilization (Labconco Corporation, Kansas City, MO, USA) and
196 used for the following analyses.

197 2.7 Size-exclusion HPLC

198 The molecular weight profiles of the gluten proteins obtained from untreated and treated wheat
199 flour samples were studied by a size-exclusion high performance liquid chromatography (HPLC)
200 according to the method of Morel et al. (2000) with some modifications. Five milligrams of freeze-
201 dried gluten sample were mixed in 150 μ L of 0.1 M sodium phosphate buffer (pH 6.9) containing
202 1% (w/v) SDS at 60 °C for 80 min to dissolve the soluble gluten proteins followed by 5 min

203 sonication. After centrifugation at $5000 \times g$ for 5 min, an aliquot of the supernatant was collected
204 for HPLC analysis. The size-exclusion HPLC was conducted on a Varian Prostar system connected
205 with a Superdex 75 10/300 GL column. To observe the size distribution, 25 μL of the sample was
206 loaded on the column and separated by an isocratic elution at a flow rate of 0.5 mL/min with 0.1
207 M sodium phosphate buffer (pH 6.9, 1.1% SDS). The detection was performed at a wavelength of
208 214 nm. The total SDS extractable protein and protein content in different molecular weight ranges
209 were calculated from the fraction areas in the chromatogram. The standard calibration curve was
210 obtained by using a series of pure standards from a gel filtration markers kit (MW 12,000-200,000
211 Da).

212 2.8 Free sulfhydryl groups (-SH)

213 Sulfhydryl groups represents one of the most vital functional groups in native proteins and it is a
214 crucial indicator for protein oxidation and crosslinking. To evaluate the protein oxidation level of
215 the wheat flour after pulsed LED treatment, the content of free -SH was evaluated as described in
216 the method by Wang et al. (2014). Briefly, 40 mg of each gluten sample was incubated with 4 mL
217 of tris-glycine buffer (pH 8.0) containing 5 mM EDTA and 2.5% (w/v) SDS with intermittent
218 vortex for 30 min, and then the -SH content was determined after the addition of Ellman's reagent
219 (5,5-dithio-bis-(2-nitrobenzoic acid). The absorbance was measured at 412 nm against the blank
220 and the calibration curve was plotted with cysteine.

221 2.9 Surface hydrophobicity

222 The surface hydrophobicity of gluten proteins from untreated and treated wheat flour samples was
223 determined as the method illustrated by Kato and Nakai (1980), using 8 mM 1-anilinonaphthalene-
224 8-sulfonic acid (ANS) in 0.1 M phosphate buffer (pH 7.0) as a fluorescent probe. The gluten
225 suspension (2 mg/ml) was prepared in 0.01 M phosphate buffer (pH 7.0) with stirring for 1.5 h at

226 20 °C, and the supernatant obtained after centrifugation (8000 × g for 20 min) was diluted with the
227 same buffer to 0.005, 0.01, 0.05, 0.1 and 0.5 mg/mL for the test. The protein concentration of the
228 supernatant was determined by the BCA assay. For the test, 20 µL of ANS solution was added into
229 1.5 mL of each diluted sample and the fluorescence intensity measured with an excitation
230 wavelength at 365 nm and an emission wavelength at 484 nm was recorded after subtracting the
231 blank with corresponding protein solution. The initial slope of the linear regression plot obtained
232 from the fluorescence intensity versus protein concentration was used as the surface
233 hydrophobicity index.

234 2.10 Water holding capacity (WHC)

235 The water holding capacity of gluten from different LED-treated (0, 30 and 60 min) wheat flour
236 was determined according to Raghavendra et al. (2004). The WHC is defined as the amount of
237 water that per gram of gluten can hold without an external force. It is an important functional
238 property of proteins, that is related to protein structures and texture of foods. Half a gram of freeze-
239 dried gluten powder was hydrated by incrementally adding distilled water while stirring. In total
240 15 mL of water was added and the gluten matrix was hydrated for 18 h at ambient temperature.
241 Then the supernatant was filtrated off on a paper towel, and the gluten residue was weighed (G_1)
242 and dried at 105 °C for 2 h (G_2). The WHC was calculated using the following equation:

$$243 \text{ WHC } \left(\frac{g_{\text{water}}}{g_{\text{dry gluten}}} \right) = \frac{G_1 - G_2}{G_2} \quad (1)$$

244 2.11 Rheological properties

245 The gluten samples were rehydrated by distilled water and kneaded with a spatula until uniform,
246 cohesive matrices formed. The gluten gels were then rested in sealed tubes at 25 °C for 2 h prior
247 to rheological analyses. The rheological analyses were performed on the Physica MCR Rheometer
248 (Anton Paar GmbH, Virginia, USA) with a 2.5 cm parallel plate at 25 °C. The dynamic rheological

249 studies were conducted in the modes of strain (γ) and frequency (ω) sweeps. The linear viscoelastic
250 region (LVR) was first determined by a strain sweep in a range of deformation from 0.01% to 100%
251 at $\omega = 10$ Hz, and then frequency sweep was operated at $\gamma=5\%$ from 0.1 to 100 Hz. The gap
252 between the parallel plate and the Peltier plate was set at 1 mm. Silicone oil was coated on the
253 edge of the sample and used to prevent the moisture change during the measurements. The changes
254 of storage modulus (elasticity, G') and loss modulus (viscosity, G'') of the samples were plotted
255 during the measurements. The ratio of these two values ($\tan \delta$, G''/G') was also recorded.

256 2.12 Protein secondary structure changes

257 The secondary structure changes of the gluten from wheat flour before and after pulsed LED
258 treatments were evaluated in hydrated gluten samples by Fourier transform infrared spectroscopy
259 (FTIR), according to the method by Nawrocka et al. (2018). The gluten samples were treated by
260 deuterium dioxide (D_2O) for 18 h at 4 °C before the analysis to avoid the interference of water
261 bands in amide I band ($1600 - 1700\text{ cm}^{-1}$), representing protein secondary structures. The spectra
262 were recorded by a Thermo Nicolet 8700 FTIR spectrometer equipped with a diamond attenuated
263 total reflectance (ATR) attachment. Spectra were scanned between 4000 and 600 cm^{-1} at 4 cm^{-1}
264 intervals and signal was averaged from 128 scans.

265 The amount of different secondary structures was estimated from relative peak areas
266 obtained in the second derivative spectra of the amide I band by using Peakfit v4.12. The peak
267 frequencies that correspond to the protein secondary structures were cited from literature (Dhaka
268 and Khatkar, 2016; Kong and Yu, 2007; Wellner et al., 2005).

269 2.13 Microstructure of gluten matrices

270 The gluten matrices were prepared as described in Section 2.11, and freeze-dried using Thermo
271 SuperModulyo freeze dryer. Fractured samples were mounted on the sample holder and then the

272 microstructure of gluten matrices was visualized under a helium-ion microscope (Zeiss Orion
273 NanoFab, Germany). The images were magnified and captured at 50 μm field of view and 10 μm
274 field of view. Eight representative pictures were captured for each sample.

275 2.14. Statistical analysis

276 The entire experiment was repeated three times and each analysis was conducted in triplicate. Data
277 were analyzed using one-way analysis of variance (ANOVA), and comparison among means was
278 assessed by conducting a studentized range test (Tukey HSD Test) at the 0.05 significance level.
279 All statistical analyses were done using SPSS statistical software (version 20.0, SPSS Inc., Chicago,
280 USA).

281 3. Results

282 3.1 Inactivation of *Salmonella* cocktail by 395 nm pulsed LED treatment

283 The disinfection effect of the 395 nm pulsed LED on *Salmonella* cocktail was examined in both
284 open and semi-closed systems (Table 1). A significant decrease in the survival of *Salmonella* was
285 noticed with the increase of the LED dosage in both open and semi-closed systems. In the open
286 system, the cell counts were reduced by 2.42 ± 0.13 log CFU/g after 60 min treatment; in the semi-
287 closed system, the cell counts were reduced by 2.91 ± 0.14 log CFU/g after 60 min. The temperature
288 increased during treatment in both systems; this increase was more pronounced in the open system.
289 Conversely, the a_w was reduced after treatment in both systems but more pronounced in the open
290 system. The reduction of the a_w corresponded to weight losses of the samples in both systems but
291 more pronounced in the open system. Although the controlled humidity (75%) and temperature
292 (25 °C) inside the semi-closed system was not able to prevent dehydration of wheat flour during
293 pulsed LED treatments, the more controlled environment inside the semi-closed system reduced
294 LED-induced drying of the flour.

295 3.2 Color changes of wheat flour after pulsed LED treatment

296 Because the bactericidal effect of treatments in the semi-closed system were higher when
297 compared to the open system, subsequent investigations on the quality of wheat flour focused on
298 samples treated inside the semi-closed system. Also, since the decontamination effect of the 10
299 min treatment was less than 2 log, only 30 min and 60 min treatments were selected for the
300 following tests. Color changes in the wheat flour before and after the pulsed LED treatments at 0,
301 30 and 60 min in the semi-closed system were evaluated by the L^* , a^* and b^* parameters (Table
302 2). A greater ($P<0.05$) L^* value was noted in the wheat flour sample after 60 min treatment
303 compared to the sample without pulsed LED treatment. The a^* values of wheat flour samples
304 increased significantly with 30 and 60 min treatments whereas the b^* value presented an opposite
305 trend, reducing significantly with extended treatment times. The results reflect that wheat flour
306 was bleached after pulsed LED treatment and showed markedly whiter, less greenness (more
307 redness) and less yellowness in contrast with the original wheat flour. The picture in supplementary
308 material showed the visual differences between the doughs made with control and the LED treated
309 samples.

310 3.3 Molecular weight distribution of gluten proteins

311 The polymerization of gluten proteins plays a key role for the baking quality of wheat flour.
312 Therefore, changes in gluten proteins after the pulsed LED treatments were evaluated by
313 determination of the molecular weight of SDS-soluble gluten proteins, by quantification of
314 sulfhydryl groups in the samples, by determination of rheological properties of wheat doughs, and
315 by FTIR. Figure 2 shows the molecular weight profiles of the SDS-soluble gluten proteins
316 extracted from wheat flour before and after the pulsed LED treatments. The molecular weight of
317 gluten proteins (Fig. 2A) was divided into four fractions: F1, from 100-350 kDa, F2, from 65-100

318 kDa, F3, from 12-65 kDa and F4, less than 12kDa. Notably, LED treatments reduced the amount
319 but increased the molecular weight of SDS-soluble gluten proteins (Fig. 2A and 2B), indicating
320 that LED treatment induced formation of larger polymers.

321 3.4 Chemical and functional properties of the gluten after pulsed LED treatment

322 3.4.1 Free sulfhydryl groups (-SH)

323 To determine whether the LED-induced polymerization of gluten proteins is mediated by oxidation
324 of sulfhydryl groups in flour, free -SH were measured in the SDS-soluble gluten proteins obtained
325 from wheat flour before and after 395 nm-LED treatments (Table 3). The content of free sulfhydryl
326 groups in gluten proteins was significantly reduced after LED treatment, with the lowest value of
327 $1.66 \pm 0.01 \mu\text{mol/g}$ protein in the sample treated for 60 min.

328 3.4.2 Surface hydrophobicity

329 The alteration of protein surface hydrophobicity is highly correlated with protein conformational
330 and functional changes, which usually points to certain level of protein denaturation and exposure
331 of hydrophobic amino acids hidden in the core of the native protein to the protein surface.
332 Variations of surface hydrophobicity of LED treated gluten samples with different treatment
333 lengths (0, 30 and 60 min) are shown in Table 3. The surface hydrophobicity was significantly
334 elevated in the gluten samples after LED treatment for 30 and 60 min, with surface hydrophobicity
335 index 11.58 ± 0.44 and 11.96 ± 0.38 , respectively.

336 3.4.3 Water holding capacity

337 Regarding to the water holding capacity (Table 3), significant differences were observed among
338 the gluten samples with and without LED treatment. The untreated gluten sample was capable of
339 absorbing and retaining more water ($1.66 \pm 0.03 \text{ g/g}$) in its three-dimensional networks when
340 compared to the samples treated with 30 and 60 min.

341 3.4.4 Rheological properties

342 To determine whether LED-induced changes in gluten quality impact their rheological properties,
343 the elastic response (storage modulus, G') and viscous response (loss modulus, G'') of SDS-
344 soluble gluten proteins were recorded in a frequency range from 0.1 to 100 Hz (Fig. 3). In general,
345 the matrix formed with gluten proteins was more solid-like, verified by higher values of G' (Fig.
346 3A) than G'' (Fig. 3B), and both of the G' and G'' were dependent on the frequency. With respect
347 to elasticity, the G' of the gluten with LED treatments showed higher values than the original
348 gluten. The G'' values, which are indicative of viscous properties, were not changed by LED
349 treatments.

350 3.5 Secondary structural changes of the treated gluten

351 The functional changes of proteins are usually ascribed to their structural changes. Therefore, it
352 was worthy to investigate the structural changes of the gluten proteins after exposure to the LED,
353 which promotes a better understanding of the effect of 395 nm pulsed LED treatment on the gluten
354 proteins. The secondary structural modifications of rehydrated gluten samples were analyzed by
355 FTIR and the obtained spectra are presented in Figure 4. Amide I bands with frequency between
356 1600 and 1700 cm^{-1} in FTIR spectrum are the most sensitive vibrational bands of protein backbone
357 that reflect the protein secondary structures (Yang et al., 2015). Based on the calculations from the
358 second derivative peaks (Table 4), the major secondary components of all the gluten samples were
359 β -sheets, accounting for over 50 % among the secondary structures, followed by α -helix and
360 random coil, and then β -turns. Similar results were reported by Li et al. (2006), a great amount of
361 β -sheet structure was found in hydrated gluten. Conformational changes were observed among the
362 hydrated gluten samples before and after the LED treatments. The percentage of intermolecular β -
363 sheet structures was significantly increased with the elevated LED treatment times, from $19.7 \pm 0.3\%$

364 in the untreated sample to $24.0\pm 0.3\%$ in the 60 min treated gluten. Significant reduction in
365 antiparallel β -sheet and α -helix and random coil structures were caused after 30 and 60 min pulsed
366 LED treatments.

367 3.6 Microstructure changes

368 To visualize the effect of the 395 nm LED on the gluten proteins, the microstructures of gluten
369 dough obtained from the 0, 30 and 60 min treatments were examined under the helium-ion
370 microscope (Fig. 5). A three-dimensional network was obtained in all the hydrated gluten samples
371 without and with different LED exposures (Fig. 5, 50 μm and 10 μm field of view). This
372 interconnected system formed by intermolecular disulphide bonds contains numerous pores that
373 can entrap water molecules and ultimately results in a viscoelastic gluten framework.

374 4. Discussion

375 The results from the inactivation study suggest the potential of using 395 nm pulsed LED treatment
376 to decontaminate *Salmonella* in low-moisture foods, particularly in a semi-closed system.
377 Although the sample temperature increased (less than 50 °C) when the LED light was applied,
378 there was no significant temperature change from 10 min to 60 min treatment time in the semi-
379 closed system. In contrast, cell counts of *Salmonella* cocktail significantly reduced during this
380 period and reached ~ 3 log reduction at 60 min with 395 nm LED treatment. It indicated the LED
381 effect was dominant than thermal effect in our study. This reduction of cell counts provides proof
382 of concept that LED at 395 nm achieves inactivation of resistant pathogens in low-moisture foods,
383 but the limited reduction of cell counts and the long treatment times necessitates further
384 optimization by change of a_w and temperature of treatment. In comparison to heat treatment, which
385 also has only a limited effect on *Salmonella* in dry foods (Finn et al., 2013), LED technology could
386 still be a potential alternative. Long treatment times between 60-240 min were required to

387 significantly reduce *Salmonella* in wheat flour at 55, 60, 65, and 70°C. For instance, 60 °C heat
388 treatment of all-purpose wheat flour for 60 min resulted in only 1.14 log CFU/g reduction in
389 *Salmonella* (Forghani et al. 2019). However, an absolute comparison in log reductions during LED
390 and heat treatments is not possible due to the different product and process conditions followed
391 and strains used in different studies. From our recent experiments, it was shown that the three
392 *Salmonella* strains used in this study i.e., FUA 1934, FUA 1946 and FUA 1955 exhibited high
393 resistance to heat treatments (Cite Bina's M.Sc. thesis – it is online already).

394 To assess the influence of the 395 nm LED on the quality of wheat flour, color changes of
395 wheat flour in the semi-closed system were evaluated after the treatments. Bleaching occurred in
396 the wheat flour under 395 nm light exposure, which may be due to the degradation of the
397 carotenoid compounds existing in wheat flour. Carotenoids are yellow-red pigments with
398 antioxidant properties (Fiedor and Burda, 2014). Lutein and zeaxanthin are the major carotenoids
399 in wheat flour (Hussain et al., 2015) and according to literature, the degradation of carotenoids
400 was mainly attributed to oxidation (Ficco et al., 2014). The possible mechanism for the bleaching
401 of wheat flour during 395 nm LED treatments could be related to the generation of ROS with the
402 aid of energy produced from photons, which interacted with the carotenoid compounds and
403 resulted in carotenoid degradation. From the picture (supplementary material), the color change
404 after LED treatments was very evident and the treated flour doughs were much less yellow
405 compared to the control flour dough. This indicated the whiter color could be visually identified
406 by consumer. Wheat flour is commonly bleached by chemicals, e.g. benzoyl peroxide, to remove
407 yellow xanthophyll and other pigments in flour to produce whiter flour and to oxidize flour
408 proteins. The result may be a good sign for industry since it means the LED could bleach the wheat

409 flour without chemicals meanwhile inactivating the microbial pathogens. However, this is also an
410 indication that oxidation happens in wheat flour during the pulsed LED treatments.

411 The oxidation occurred during the LED treatments was verified by the molecular weight
412 migration from low to high molecular weight gluten proteins in the treated samples as presented
413 in the section 3.3. The formation of bigger polymers was also observed by the total areas and the
414 fraction areas (Fig. 2B). Crosslinking of gluten proteins by disulfide-bonds decreases the SDS-
415 extractable proteins in wheat (Pomeranz, 2012). Accordingly, the size distribution and the amount
416 of SDS-soluble proteins from untreated and LED-treated wheat flour imply that the LED-induced
417 oxidation occurred in the wheat gluten with 30 and 60 min treatment, which accelerated the
418 generation of the disulfide bonds inter or intra the gluten proteins, therefore caused the higher
419 degree of crosslinking and large polymers formation.

420 The results about the chemical and functional properties of the gluten after 395 nm LED
421 treatment provided more evidence for oxidation. The reduced amount of -SH presented in section
422 3.4.1 implicated more free -SH groups were oxidized into S-S bonds to form crosslinking with the
423 extended period of LED treatment. The phenomenon of increased surface hydrophobicity after the
424 LED exposure also implies the oxidative modifications occurred in gluten proteins. The native
425 proteins were unfolded, exposed the hydrophobic amino acids and further formed covalently cross-
426 linked protein aggregates. Gluten proteins are rich in hydrophobic amino acids, for instance,
427 glycine, proline and glutamine, the greater exposure of these side chains will lead to more
428 hydrophobic interactions, which is considered to play an important role in stabilizing gluten
429 structure as well as baking and rheological properties of dough (Ponte et al., 2000). The
430 development of gluten matrix involves protein-protein and protein-water interactions. Hydrated
431 glutenins and gliadins tend to align and form crosslinks (disulfide bonds) among glutenin

432 molecules and between glutenin and gliadin molecules during mixing, leading to the generation of
433 the interconnected network in which the water molecules are entrapped (MaCann and Day, 2013).
434 However, prior to mixing, the pre-developed crosslinking structures resulted from the LED light
435 may interfere the interaction of protein with water during kneading, thus less uniform network
436 could be formed, and lower amount of water were retained in the protein structure (section 3.4.3).
437 Besides, the increase in surface hydrophobicity caused certain degree of protein aggregation that
438 may also make the proteins less accessible for water molecules.

439 The increase in the mechanical strength of the gluten formed gels (described in the section
440 3.4.4) may be the consequences of the addition of crosslinked structures after LED-induced
441 oxidation, which provided greater level of gel elasticity. Monomeric low molecular weight (LMW)
442 gliadins only have intrachain disulfide bonds while the polymeric high molecular weight (HMW)
443 glutenin subunits have both intra- and interchain bonds, therefore the polymeric glutenin subunits
444 own higher chances to enter the polymerization reactions and act as “chain extender”, to produce
445 more cross-linked conformations. The gliadins and glutathione are found to be terminators of the
446 chains (Wieser, 2007). The molecular weight distribution of the gluten samples (section 3.3) has
447 illustrated a shift from the monomers to polymers and HMW subunits during LED treatment. The
448 presence of larger amounts of the HMW subunits may subsequently involve in more
449 polymerization reactions during mixing and form more crosslinked networks that eventually work
450 for a stronger matrix in the LED treated samples. In terms of the viscosity, there was no evident
451 changes among the different gluten samples, indicating the LED-induced oxidation had dominant
452 effects on the elastic properties rather than viscous properties of the gluten matrix. Moreover, the
453 higher surface hydrophobicity found in the LED treated samples may stimulate more hydrophobic
454 interactions that consequently provide support to the gluten framework. In the case of dough

455 making or bread making, oxidation is favored during mixing for the formation of large glutenin
456 polymers to obtain an elastic dough. The results indicate that 395 nm LED light can accelerate the
457 mixing process and assist to produce a dough with higher resilience that would positively impact
458 on the quality of the final products (i.e. baking products).

459 The structural changes of the gluten proteins are highly associated with the functional
460 changes after the LED treatments. The α -helix has been linked as a characteristic for gliadins
461 (Wang et al., 2014), which may be diminished due to the involvement of gliadins into forming the
462 large polymers after LED oxidation. Since β -turns are mostly exposed on protein surface, the
463 dramatic increase of the β -turn structures in the gluten samples after 60 min LED exposure may
464 be correlated to the alteration of the surface hydrophobicity by LED as shown in section 3.4.2
465 Greater occurrence of intermolecular β -sheet structures in the gluten samples has been related to
466 the interactions between glutenin subunits (Popineau et al., 1994). The increased amounts of β -
467 turns and β -sheets in gluten after the LED treatments played important roles on elasticity and
468 stability in gluten network, which is an essential property of gluten for good bread making (Dhaka
469 and Khatkar 2016). This is in agreement with the result that large polymers formed in gluten after
470 exposure to the LED through disulfide linking between glutenin subunits and led to higher elastic
471 gluten matrixes.

472 In conclusion, the 395 nm pulsed LED treatment is a promising decontamination approach
473 for wheat flour, since it brings multiple benefits. A maximum 2.91 log reduction of *Salmonella*
474 cocktail was obtained in wheat flour treated with 395 nm pulsed LED for 60 min in a semi-closed
475 system. The 395 nm LED treatments also led to oxidation in wheat flour which subsequently
476 resulted in bleaching, and polymerization of gluten components through disulphide linkage. The
477 contents of protein secondary structures were altered significantly after pulsed LED treatment, but

478 the rheological properties were not deteriorated. The LED-induced oxidation bleached the flour
479 components without chemicals, and cross-linked gluten polymers, which may promote the
480 efficiency of the dough mixing process and lead to better viscoelastic baking products. However,
481 commercial application of the pulsed LED technology requires process time reduction and LED
482 disinfection efficacy maximization (maybe through a better a_w control and a treatment system with
483 vibratory platform for better light exposure of wheat flour), and improvement in the methods for
484 controlling the extent of crosslinking formation to get required wheat flour product quality. By
485 addressing these challenges, novel food decontamination and drying processes using pulsed LEDs
486 for variety of foods can be possibly developed in the future.

487 **Acknowledgements**

488 We acknowledge the funding support (Grant number 2018F040R) from Alberta Agriculture and
489 Forestry. The authors would like to thank P&H Milling Group (Lethbridge, AB, Canada) for
490 providing the wheat flour. The authors wish to extend appreciation to Dr. Mirko Betti for the access
491 to the rheometer.

492

493

494 **References**

495 Annual report of CDC (2015) <https://www.cdc.gov/foodnet/pdfs/FoodNet-Annual-Report-2015->

496 [508c.pdf](#), accessed on Nov 25th, 2018.

497

498 Archer, J., Jervis, E. T., Bird, J., Gaze, J. E. (1998). Heat resistance of *Salmonella* Weltevreden in
499 low-moisture environments. *Journal of Food Protection*, 61(8), 969–973.

500

501 Bari, M. L., Nei, D., Sotome, I., Nishina, I., Isobe, S., & Kawamoto, S. (2009). Effectiveness of
502 sanitizers, dry heat, hot water, and gas catalytic infrared heat treatments to inactivate *Salmonella*
503 on almonds. *Foodborne Pathogens and Diseases*, 6(8), 953–958.

504

505 Beck, S. E., Rodriguez, R. A., Hawkins, M. A., Hargy, T. M., Larason, T. C., & Linden, K. G.
506 (2015). Comparison of UV-induced inactivation and RNA damage in MS2 phage across the
507 germicidal UV spectrum. *Applied and Environmental Microbiology*, 82(5), pp.1468-1474.
508 <http://doi: 10.1128/AEM.02773-15>

509

510 Beuchat, L. R., Komitopoulou, E., Beckers, H., Betts, R. P., Bourdichon, F., & Fanning, S. et al.

511 (2013). Low–water activity foods: Increased concern as vehicles of foodborne pathogens. *Journal*

512 *of Food Protection*, 76(1), 150-172. <http://doi: 10.4315/0362-028x.jfp-12-211>

513

514 Bintsis, Thomas, Litopoulou-Tzanetaki, E., & Robinson, R. K. (2000). Existing and potential

515 applications of ultraviolet light in the food industry - a critical review. *Journal of the Science of*

516 *Food and Agriculture*, 80(6), 637–645. [https://doi.org/10.1002/\(SICI\)1097-](https://doi.org/10.1002/(SICI)1097-)

517 [0010\(20000501\)80:6<637::AID-JSFA603>3.0.CO;2-1](https://doi.org/10.1002/(SICI)1097-0010(20000501)80:6<637::AID-JSFA603>3.0.CO;2-1)

518

519 Centers of Disease Control and Prevention (1998). Multistate outbreak of *Salmonella* serotype
520 Agona infections linked to toasted oats cereal--United States, April-May. *Morbidity and Mortality*
521 *Weekly Report*. 47(22), 462-4.

522

523. Clyde E. Stauffer. (2007). Chapter 11: Principle of dough formation. In S. P. Cauvain,
524. & L. S. Young (Eds.), *Technology of Breadmaking*. Berlin: Springer Science+Business Media,
525 LLC.

526.

527 Dai, T., Vrahas, M. S., Murray, C. K., & Hamblin, M. R. (2012). Ultraviolet C irradiation: an
528 alternative antimicrobial approach to localized infections? *Expert Review of Anti-Infective Therapy*,
529 *10*(2), 185–195. <https://doi.org/10.1586/eri.11.166>

530

531 Danyluk, M. D., Uesugi, A. R., Harris, L. J. (2005). Survival of *Salmonella enteritidis* PT 30 on
532 inoculated almonds after commercial fumigation with propylene oxide. *Journal of Food*
533 *Protection*. *68*, 1613–1622.

534

535 de Oliveira, E. F., Cossu, A., Tikekar, R. V., & Nitin, N. (2017). Enhanced antimicrobial activity
536 based on a synergistic combination of sublethal levels of stresses induced by UV-A light and
537 organic acids. *Applied and Environmental Microbiology*, *83*(11).
538 <https://doi.org/10.1128/AEM.00383-17>

539

540 Dhaka, V., & Khatkar, B. S. (2016). Microstructural, thermal and IR spectroscopy characterisation
541 of wheat gluten and its sub fractions. *Journal of Food Science and Technology*, *53*(8), 3356–3363.
542 <https://doi.org/10.1007/s13197-016-2314-9>

543

544 FDA (2017). *Raw dough's a raw deal and could make you sick*.
545 [https://www.fda.gov/consumers/consumer-updates/raw-doughs-raw-deal-and-could-make-you-](https://www.fda.gov/consumers/consumer-updates/raw-doughs-raw-deal-and-could-make-you-sick/)
546 [sick/](https://www.fda.gov/consumers/consumer-updates/raw-doughs-raw-deal-and-could-make-you-sick/) Accessed 31 August 2019.

547

548

549 FDA (2019). *Hometown food company recalls two production lot codes of Pillsbury® Unbleached*
550 *All-Purpose 5lb flour due to possible health risk*. [https://www.fda.gov/safety/recalls-market-](https://www.fda.gov/safety/recalls-market-withdrawals-safety-alerts/hometown-food-company-recalls-two-production-lot-codes-pillsbury-unbleached-all-purpose-5lb-flour/)
551 [withdrawals-safety-alerts/hometown-food-company-recalls-two-production-lot-codes-pillsburyr-](https://www.fda.gov/safety/recalls-market-withdrawals-safety-alerts/hometown-food-company-recalls-two-production-lot-codes-pillsbury-unbleached-all-purpose-5lb-flour/)
552 [unbleached-all-purpose-5lb-flour/](https://www.fda.gov/safety/recalls-market-withdrawals-safety-alerts/hometown-food-company-recalls-two-production-lot-codes-pillsbury-unbleached-all-purpose-5lb-flour/) Accessed 31 August 2019.
553

554 Ficco, D. B. M., Mastrangelo, A. M., Trono, D., Borrelli, G. M., De Vita, P., Fares, C., & et al.
555 (2014). The colours of durum wheat: a review. *Crop and Pasture Science*, 65(1), 1.
556 <https://doi.org/10.1071/CP13293>

557

558 Fiedor, J., & Burda, K. (2014). Potential role of carotenoids as antioxidants in human health and
559 disease. *Nutrients*, 6(2), 466–488. <https://doi.org/10.3390/nu6020466>

560

561 Finn, S., Condell, O., McClure, P., Amézquita, A., & Fanning, S. (2013). Mechanisms of survival,
562 responses, and sources of *Salmonella* in low-moisture environments. *Frontiers in Microbiology*,
563 4(331). 1-14. [doi: 10.3389/fmicb.2013.00331](https://doi.org/10.3389/fmicb.2013.00331)

564

565 Forghani, F., den Bakker, M., Liao, J., Payton, A., Futral, A. N., & Diez-Gonzalez, F. (2019).
566 *Salmonella* and enterohemorrhagic *Escherichia coli* serogroups O45, O121, O145 in wheat flour:
567 Effects of long-term storage and thermal treatments. *Frontiers in Microbiology*, 10, 323-333.

568 <https://doi.org/10.3389/fmicb.2019.00323>

569

570 Government of Canada (2016). [https://www.canada.ca/en/public-health/services/food-borne-](https://www.canada.ca/en/public-health/services/food-borne-illness-canada/yearly-food-borne-illness-estimates-canada.html)
571 [illness-canada/yearly-food-borne-illness-estimates-canada.html](https://www.canada.ca/en/public-health/services/food-borne-illness-canada/yearly-food-borne-illness-estimates-canada.html) , accessed on Nov 25th, 2018.

572

573 Haughton, P. N., Grau, E. G., Lyng, J., Cronin, D., Fanning, S., & Whyte, P. (2012). Susceptibility
574 of *Campylobacter* to high intensity near ultraviolet/visible 395±5nm light and its effectiveness for
575 the decontamination of raw chicken and contact surfaces. *International Journal of Food*
576 *Microbiology*, 159(3), 267–273. <https://doi.org/10.1016/j.ijfoodmicro.2012.09.006>

577

578 Hussain, A., Larsson, H., Kuktaite, R., Olsson, M. E., & Johansson, E. (2015). Carotenoid content
579 in organically produced wheat: relevance for human nutritional health on consumption.
580 *International Journal of Environmental Research and Public Health*, 12(11), 14068–14083.
581 <https://doi.org/10.3390/ijerph121114068>

582

583 Karran, P., & Brem, R. (2016). Protein oxidation, UVA and human DNA repair. *DNA Repair*, 44,
584 178–185. <https://doi.org/10.1016/j.dnarep.2016.05.024>

585

586 Kato, A., & Nakai, S. (1980). Hydrophobicity determined by a fluorescence probe method and its
587 correlation with surface properties of proteins. *Biochimica et Biophysica Acta (BBA) - Protein*
588 *Structure*, 624(1), 13–20. [https://doi.org/10.1016/0005-2795\(80\)90220-2](https://doi.org/10.1016/0005-2795(80)90220-2)

589

590 Kieffer, R., Schurer, F., Köhler, P., & Wieser, H. (2007). Effect of hydrostatic pressure and
591 temperature on the chemical and functional properties of wheat gluten: Studies on gluten, gliadin
592 and glutenin. *Journal of Cereal Science*, 45(3), 285–292. <https://doi.org/10.1016/j.jcs.2006.09.008>

593

594 Kong, J., & Yu, S. (2007). Fourier transform infrared spectroscopic analysis of protein secondary
595 structures. *Acta Biochimica et Biophysica Sinica*, 39(8), 549–559. [https://doi.org/10.1111/j.1745-](https://doi.org/10.1111/j.1745-7270.2007.00320.x)
596 [7270.2007.00320.x](https://doi.org/10.1111/j.1745-7270.2007.00320.x)

597 Li, W., Dobraszczyk, B., Dias, A., & Gil, A. (2006). Polymer conformation structure of wheat
598 proteins and gluten subfractions revealed by ATR-FTIR. *Cereal Chemistry Journal*, 83(4), 407-
599 410. [http://doi: 10.1094/cc-83-0407](http://doi:10.1094/cc-83-0407)

600

601 Liu, S., Ozturk, S., Xu, J., Kong, F., Gray, P., Zhu, M. J., ... Tang, J. (2018). Microbial validation
602 of radio frequency pasteurization of wheat flour by inoculated pack studies. *Journal of Food*
603 *Engineering*, 217, 68–74. <https://doi.org/10.1016/j.jfoodeng.2017.08.013>

604

605 McCallum, L., Paine, S., Sexton, K., Dufour, M., Dyet, K., Wilson, M., Campbell, D.,
606 Bandaranayake, D., & Hope, V. (2013). An outbreak of *Salmonella* Typhimurium phage type 42
607 associated with the consumption of raw flour. *Foodborne Pathogens and Disease*. 10(2), 159-64.
608

609 McCann, T. H., & Day, L. (2013). Effect of sodium chloride on gluten network formation, dough
610 microstructure and rheology in relation to breadmaking. *Journal of Cereal Science*, 57(3), 444–
611 452. <https://doi.org/10.1016/j.jcs.2013.01.011>

612

613 [Mercer, R.M., Walker, B.D., Yang, X., McMullen, L.M., Gänzle, M.G. \(2017\). The locus of heat](https://doi.org/10.1016/j.jcs.2013.01.011)
614 [resistance \(LHR\) mediates heat resistance in *Salmonella enterica*, *Escherichia coli* and](https://doi.org/10.1016/j.jcs.2013.01.011)
615 [*Enterobacter cloacae*. *Food Microbiology*. 64, 96-103.](https://doi.org/10.1016/j.jcs.2013.01.011)

616

617

618 Morel, M. H., Dehlon, P., Autran, J. C., Leygue, J. P., & Bar-L'Helgouac'h, C. (2000). Effects of
619 temperature, sonication time, and power settings on size distribution and extractability of total
620 wheat flour proteins as determined by size-exclusion high-performance liquid chromatography.
621 *Cereal Chemistry Journal*, 77(5), 685–691. <https://doi.org/10.1094/CCHEM.2000.77.5.685>

622

623 Myoda, S. P., Gilbreth, S., Akins-Lewenthal, D., Davidson, S. K., & Samadpour, M. (2019)
624 Occurrence and levels of *Salmonella*, enterohemorrhagic *Escherichia coli*, and *Listeria* in raw
625 wheat. *Journal of Food Protection*, 82(6), 1022-1027. [https://doi.org/10.4315/0362-028X.JFP-18-](https://doi.org/10.4315/0362-028X.JFP-18-345)
626 [345](https://doi.org/10.4315/0362-028X.JFP-18-345).

627

628 Ng, H., Bayne, H.G., Garibaldi, J.A., (1969). Heat resistance of *Salmonella*: the uniqueness of
629 *Salmonella* Senftenberg 755W. *Applied Microbiology* 17, 78-82.

630

631

632 Pomeranz, Y. (2012). Chapter 5: Protein generals. In *Functional Properties of Food Components*
633 (p. 175). Cambridge: Academic Press.

634

635 Ponte, J. G., Dogan, I. S., & Kulp, K. (2000). Chapter 27: Special food ingredients from cereals.
636 In K. Kulp (Ed.), *Handbook of Cereal Science and Technology* (2nd ed., p. 756). Boca Raton: CRC
637 Press.

638

639 Popineau, Y., Bonenfant, S., Cornec, M., & Pezolet, M. (1994). A study by infrared spectroscopy
640 of the conformations of gluten proteins differing in their gliadin and glutenin compositions.
641 *Journal of Cereal Science*, 20(1), 15–22. <https://doi.org/10.1006/jcrs.1994.1040>
642

643 Raghavendra, S. N., Rastogi, N. K., Raghavarao, K. S. M. S., & Tharanathan, R. N. (2004). Dietary
644 fiber from coconut residue: effects of different treatments and particle size on the hydration
645 properties. *European Food Research and Technology*, 218(6), 563–567.
646 <https://doi.org/10.1007/s00217-004-0889-2>
647

648 Rastogi, R. P., Richa, Kumar, A., Tyagi, M. B., & Sinha, R. P. (2010). Molecular mechanisms of
649 ultraviolet radiation-induced DNA damage and repair. *Journal of Nucleic Acids*, 2010, 1–32.
650 <https://doi.org/10.4061/2010/592980>
651

652 Schubert, E. F. (2003). *Light-emitting diodes*. UK: Cambridge University Press.
653

654 Shin, J.-Y., Kim, S.-J., Kim, D.-K., & Kang, D.-H. (2016). Fundamental characteristics of deep-
655 UV light-emitting diodes and their application to control foodborne pathogens. *Applied and*
656 *Environmental Microbiology*, 82(1), 2–10. <https://doi.org/10.1128/AEM.01186-15>
657

658 Shirai, A., Watanabe, T., & Matsuki, H. (2017). Inactivation of foodborne pathogenic and spoilage
659 micro-organisms using ultraviolet-A light in combination with ferulic acid. *Letters in Applied*
660 *Microbiology*, 64(2), 96–102. <https://doi.org/10.1111/lam.12701>
661

662 Wieser, H. (2007). Chemistry of gluten proteins. *Food Microbiology*, 24(2), 115-119.
663 <http://doi.org/10.1016/j.fm.2006.07.004>
664

665 Syamaladevi, R. M., Tang, J., Villa-Rojas, R., Sablani, S., Carter, B., & Campbell, G. (2016a).
666 Influence of water activity on thermal resistance of microorganisms in low-moisture foods: A
667 Review. *Comprehensive Reviews In Food Science And Food Safety*, 15(2), 353-370. [http://doi:](http://doi:10.1111/1541-4337.12190)
668 [10.1111/1541-4337.12190](http://doi:10.1111/1541-4337.12190)
669

670 Syamaladevi, R.M., Tadapaneni, R., Xu, J., Villa-Rojas, R., Tang, J., Carter, B. et al. (2016b).
671 Water activity change at elevated temperatures and thermal resistance of *Salmonella* in all purpose
672 wheat flour and peanut butter. *Food Research International*, 81, 163-170. [http://doi:](http://doi:10.1016/j.foodres.2016.01.008)
673 [10.1016/j.foodres.2016.01.008](http://doi:10.1016/j.foodres.2016.01.008)
674

675 Tack, D. M., Marder, E. P., Griffin, P. M., et al. (2019) Preliminary Incidence and Trends of
676 Infections with Pathogens Transmitted Commonly Through Food — Foodborne Diseases Active
677 Surveillance Network, U.S. Sites, 2015–2018. *Morbidity and Mortality Weekly Report*, 68, 369–
678 373. <http://dx.doi.org/10.15585/mmwr.mm6816a2>
679

680 Wang, P., Chen, H., Mohanad, B., Xu, L., Ning, Y., Xu, J. et al. (2014). Effect of frozen storage
681 on physico-chemistry of wheat gluten proteins: Studies on gluten-, glutenin- and gliadin-rich
682 fractions. *Food Hydrocolloids*, 39, 187–194. <https://doi.org/10.1016/j.foodhyd.2014.01.009>
683

684 Wang, P., Xu, L., Nikoo, M., Ocen, D., Wu, F., Yang, N., ... Xu, X. (2014). Effect of frozen
685 storage on the conformational, thermal and microscopic properties of gluten: Comparative studies
686 on gluten-, glutenin- and gliadin-rich fractions. *Food Hydrocolloids*, 35, 238–246.
687 <https://doi.org/10.1016/j.foodhyd.2013.05.015>
688

689 Wang, Q., de Oliveira, E. F., Alborzi, S., Bastarrachea, L. J., & Tikekar, R. V. (2017). On
690 mechanism behind UV-A light enhanced antibacterial activity of gallic acid and propyl gallate
691 against Escherichia coli O157:H7. *Scientific Reports*, 7(1). [https://doi.org/10.1038/s41598-017-](https://doi.org/10.1038/s41598-017-08449-1)
692 [08449-1](https://doi.org/10.1038/s41598-017-08449-1)
693

694 Wellner, N., Mills, E. N. C., Brownsey, G., Wilson, R. H., Brown, N., Freeman, J., ... Belton, P.
695 S. (2005). Changes in protein secondary structure during gluten deformation studied by dynamic
696 Fourier transform infrared spectroscopy. *Biomacromolecules*, 6(1), 255–261.
697 <https://doi.org/10.1021/bm049584d>
698

699 Wieser, H. (2007). Chemistry of gluten proteins. *Food Microbiology*, 24(2), 115-119.
700

701 Yang, H., Yang, S., Kong, J., Dong, A., & Yu, S. (2015). Obtaining information about protein
702 secondary structures in aqueous solution using Fourier transform IR spectroscopy. *Nature*
703 *Protocols*, 10(3), 382-396. doi: 10.1038/nprot.2015.024
704
705

Table 1

Inactivation of the *Salmonella* cocktail after different LED treatment times at 395 nm in both open and semi-closed systems (RH=75%, T=25 °C), as well as the changes in sample temperature, weight loss and water activity.

Treatment time (min)	Dose (J/cm ²)	Reduction of viable cell counts (log CFU/g)		Sample Temperature (°C)		Weight Loss (%)		Water activity	
		open	semi-closed	open	semi-closed	open	semi-closed	open	semi-closed
10	270	0.89±0.07 ^c	1.49±0.17 ^{c*}	51.3±0.6 ^{b*}	47.7±0.6 ^a	1.39±0.03 ^{b*}	1.10±0.10 ^a	0.11±0.00 ^a	0.22±0.00 ^{a*}
30	810	1.95±0.04 ^b	2.23±0.18 ^b	52.3±0.6 ^{ab*}	48±1.0 ^a	1.53±0.18 ^b	1.17±0.06 ^a	0.11±0.00 ^{ab}	0.21±0.00 ^{b*}
60	1620	2.42±0.13 ^a	2.91±0.14 ^{a*}	53.0±0.0 ^{a*}	48.7±0.6 ^a	1.88±0.03 ^{a*}	1.20±0.00 ^a	0.10±0.00 ^b	0.20±0.00 ^{b*}

Values are given as mean ± standard deviation (n = 3).

Different letters in the same column indicate significant (p < 0.05) differences between the means.

Asterisk (*) indicates a significant difference between the open and the semi-closed systems.

Table 2

Color changes of the wheat flour before and after different LED treatment times at 395 nm in the semi-closed system (RH=75%, T=25 °C).

Treatment time (min)	L* (lightness)	a* (greenness and redness)	b* (blueness and yellowness)
0 min	92.37±0.67 ^b	-1.48±0.03 ^c	13.4±0.70 ^a
30 min	93.32±1.29 ^{ab}	-0.69±0.09 ^b	7.8±0.87 ^b
60 min	93.76±0.40 ^a	-0.47±0.03 ^a	6.4±0.18 ^c

Values are given as mean ± standard deviation (n = 3).

Different letters in the same column indicate significant ($p < 0.05$) differences between the means.

Table 3

Functional properties of gluten obtained from wheat flour before and after different LED treatment times at 395 nm in the semi-closed system (RH=75%, T=25 °C).

Treatment time (min)	Free -SH ($\mu\text{mol/g}$ protein)	Surface hydrophobicity index	Water holding capacity (g/g)
0 min	2.88 \pm 0.17 ^a	7.43 \pm 0.45 ^b	1.66 \pm 0.03 ^a
30 min	2.22 \pm 0.02 ^b	11.58 \pm 0.44 ^a	1.50 \pm 0.04 ^b
60 min	1.66 \pm 0.01 ^c	11.96 \pm 0.38 ^a	1.48 \pm 0.04 ^b

Values are given as mean \pm standard deviation (n = 3).

Different letters in the same column indicate significant ($p < 0.05$) differences between the means.

Table 4

Secondary structures of hydrated gluten obtained from wheat flour before and after different LED treatment times at 395 nm in the semi-closed system (RH=75%, T=25 °C).

Treatment time (min)	Gluten Secondary Structures (%)				
	Intermolecular β -sheet (%) (1615 \pm 2 cm ⁻¹)	Antiparallel β -sheet (%) (1633 \pm 2 cm ⁻¹)	α -helix and random coil (%) (1650 \pm 2 cm ⁻¹)	β -turns (%) (1666 \pm 3 cm ⁻¹)	β -turns (%) (1683 \pm 3 cm ⁻¹)
0	19.7 \pm 0.3 ^c	35.6 \pm 0.6 ^a	28.1 \pm 0.4 ^a	11.3 \pm 0.1 ^b	5.3 \pm 0.1 ^b
30	22.3 \pm 0.3 ^b	31.7 \pm 0.6 ^b	26.0 \pm 0.4 ^b	14.4 \pm 0.3 ^a	5.5 \pm 0.1 ^b
60	24.0 \pm 0.3 ^a	28.4 \pm 0.5 ^c	24.3 \pm 0.4 ^c	15.6 \pm 0.3 ^a	7.6 \pm 0.1 ^a

Values are estimated from the second derivative peak areas of the FTIR spectra from 1600 to 1700 cm⁻¹.

Values are given as mean \pm standard deviation (n = 3).

Different letters in the same column indicate significant (p < 0.05) differences between the means

Figure captions

Figure 1. Molecular weight profiles of the gluten obtained from wheat flour before and after different LED treatment times at 395 nm in the semi-closed system (RH=75%, T=25 °C). A: Size distribution chromatograph of the gluten samples and the peak fractions (F1: 100-350 kDa; F2: 65-100 kDa; F3: 12-65 kDa; F4: <12kDa). B: Total areas and fraction areas of the peaks eluted.

Figure 2. Frequency sweeps of storage modulus G' (A) and loss modulus G'' (B) for gluten samples obtained from wheat flour before and after different LED treatment times at 395 nm in the semi-closed system (RH=75%, T=25 °C).

Figure 3. FTIR spectra of hydrated gluten samples obtained from wheat flour before and after different LED treatment times at 395 nm in the semi-closed system (RH=75%, T=25 °C).

Figure 4. Microstructural images of hydrated gluten samples obtained from wheat flour before and after different 395 nm-LED treatments in the semi-closed system (RH=75%, T=25 °C) at different magnifications.

Figure 1

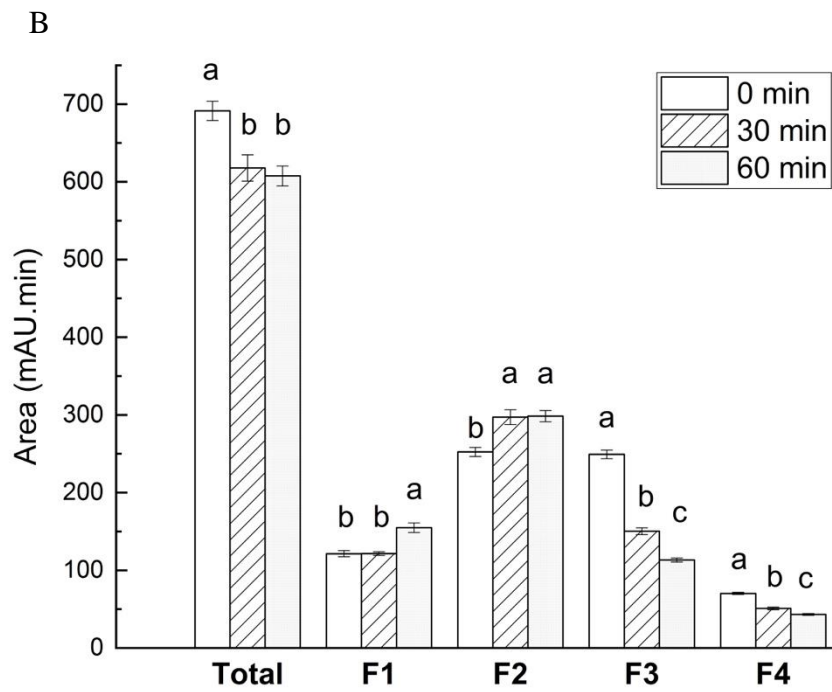
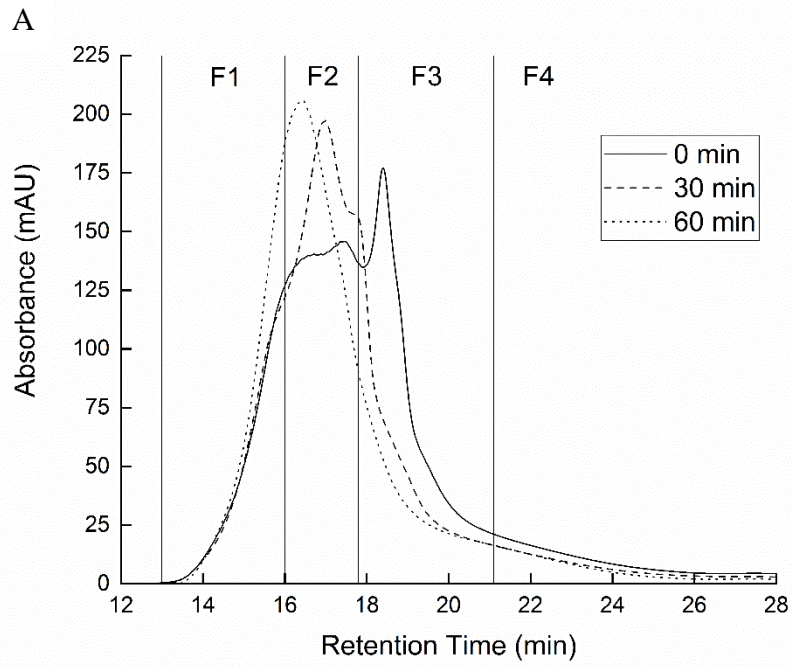


Figure 2

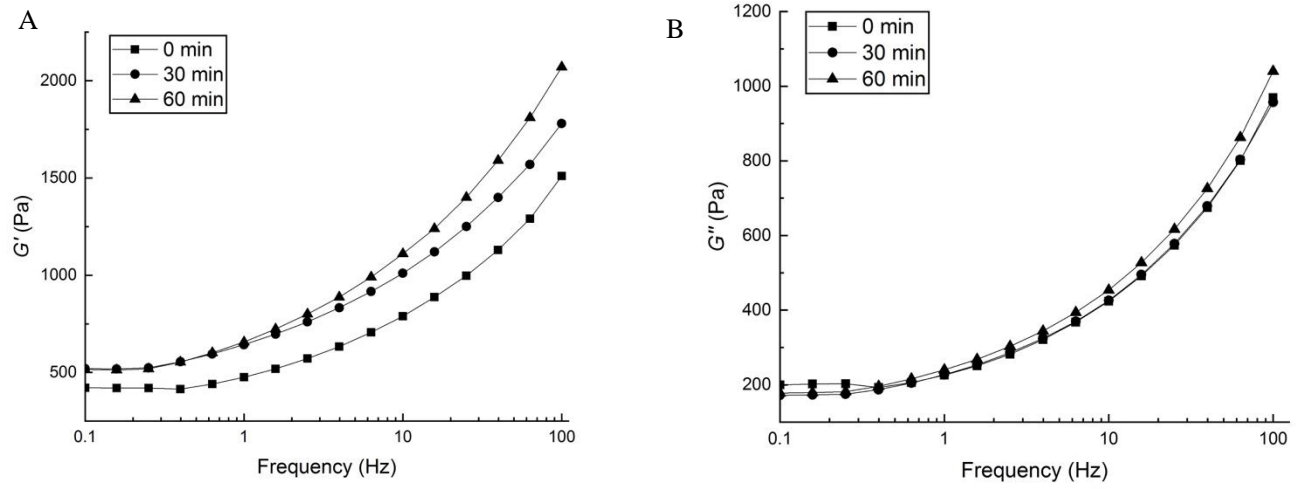


Figure 3

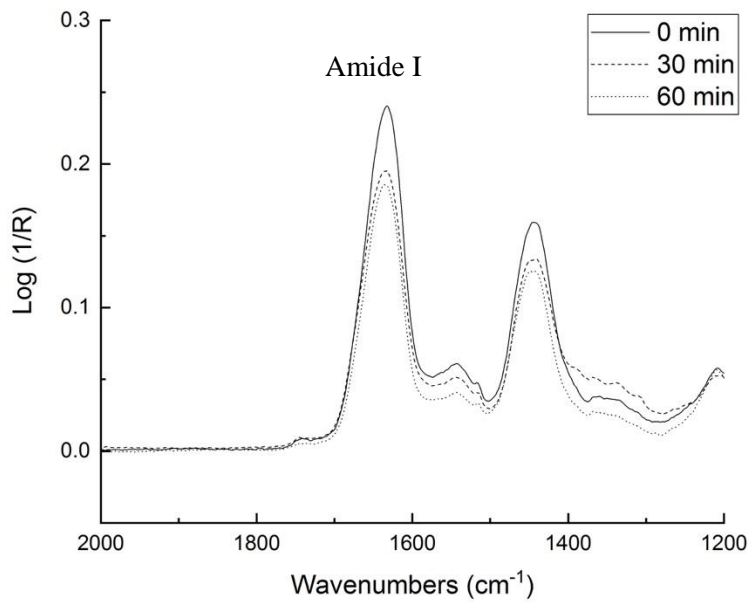


Figure 4

